Water flux estimates from a Belgian Scots pine stand: a comparison of different approaches

L. Meiresonne[a,*], D.A. Sampson[b,1], A.S. Kowalski[b], I.A. Janssens[b], N. Nadezhdina[c], J. Cermák[c], J. Van Slycken[a], R. Ceulemans[b]

[a]*Institute for Forestry and Game Management (IBW), Ministry of the Flemish Community, Gaverstraat 4, B-9500 Geraardsbergen, Belgium*
[b]*Department of Biology, University of Antwerpen (UIA), Universiteitsplein 1, B-2610 Wilrijk, Belgium*
[c]*Institute of Forest Ecology, Faculty of Forestry and Wood technology, Mendel University of Agriculture and Forestry, Zemedelska 3, CS-61300 Brno, Czech Republic*

Abstract

Four distinct approaches, that vary markedly in the spatial and temporal resolution of their measurement and process-level outputs, are used to investigate the daily and seasonal water vapour exchange in a 70-year-old Belgian Scots pine forest. Transpiration, canopy interception, soil evaporation and evapotranspiration are simulated, using a stand-level process model (SECRETS) and a soil water balance model (WAVE). Simulated transpiration was compared with up-scaled sap flow measurements and simulated evapotranspiration to eddy covariance measurements.

Reasonable agreement in the temporal trends and in the annual water balance between the two models was observed, however daily and weekly predictions often diverged. Most notably, WAVE estimated very low, to no transpiration during late autumn, winter and early spring when incident radiation fell below ~ 50 W m^{-2} while SECRETS simulated low ($0.1-0.4$ mm day^{-1}) fluxes during the same period. Both models exhibited similar daily trends in simulated transpiration when compared with sap flow estimates, although simulations from SECRETS were more closely aligned. In contrast, WAVE over-estimated transpiration during periods of no rainfall and under-estimated transpiration during rainfall. Yearly, total evapotranspiration simulated by the models were similar, i.e. 658 mm (1997) and 632 mm (1998) for WAVE and 567 mm (1997) and 619 mm (1998) for SECRETS.

Maximum weekly-average evapotranspiration for WAVE exceeded 5 mm day^{-1}, while SECRETS never exceeded 4 mm day^{-1}. Both models, in general, simulated higher evapotranspiration than that measured with the eddy covariance technique. An impact of the soil water content in the direct relationship between the models and the eddy covariance measurements was found.

The results suggest that: (1) different model formulations can reproduce similar results depending on the scale at which outputs are resolved, (2) SECRETS estimates of transpiration were well correlated with the empirical measurements, and (3) neither model fitted favourably to the eddy covariance technique.
© 2002 Elsevier Science B.V. All rights reserved.

Keywords: Evapotranspiration; Modelling; Sap flow; Eddy covariance; Transpiration; Scots pine

---

* Corresponding author. Tel.: +32-54-437-118; fax: +32-54-436-160.
  E-mail address: linda.meiresonne@lin.vlaanderen.be (L. Meiresonne).
  [1] Present address: Virginia Polytechnic Institute and State University in cooperation with the USDA Forest Service, 3041 Cornwallis Road, Research triangle Park, North Carolina, USA 27709.

1. Introduction

Transpiration and evaporation of water by vegetation are important components of the energy exchange at the earth's surface. Forests contribute substantially to the total energy budget, as they cover large areas of the planet. Analytical studies of forest evapotranspiration, in conjunction with modelling, are therefore important (Rutter et al., 1975; McNaughton and Jarvis, 1983; Stewart, 1984, 1988; Jarvis, 1985). Many different disciplines (e.g. plant physiology, ecology, meteorology, hydrology and soil science) have been developing models to estimate water vapour exchange in forests. Different approaches and methodologies are often used, depending on the focus and interest of each discipline varies. The variety of approaches has generated the development of many different forest water flux models. In addition to discipline-specific influence on model development, other factors influenced model structure and design such as the modelling objectives, the spatial and temporal scales of interest and the availability of data to parameterise the models used (Dekker et al., 2000). Single-layer, multi-layer and three-dimensional models have been developed over the past decades, simulating transpiration and evaporation at local, regional and global scales (Raupach and Finnigan, 1988). As interception and evaporation of rainfall are also important hydrological processes in forest ecosystems, several physically based (Rutter et al., 1971; Gash, 1979; Loustau et al., 1992a,b) and stochastic models (Stewart, 1984; Calder, 1986) have been developed to simulate throughfall, evaporation and canopy storage.

In addition to this wide variety of models, other techniques can be used to estimate the exchange of water vapour between canopies and the atmosphere. Reliable, direct measurements of forest transpiration are, however, lacking. Direct measurements of sap flow can be scaled up from the individual tree to the stand level using biometric scaling factors such as projected crown area, leaf area, basal area, timber volume and others (Cermák, 1989; Cermák and Kucera, 1990). However, these stand-level transpiration rates are strongly dependent on the up-scaling process. Presently, canopy level evapotranspiration by forests is measured with the eddy covariance technique at many sites around the world (Baldocchi et al., 1996; Valentini et al., 2000), but these measurements are also subject to large uncertainties (see further).

In this contribution four different approaches-from the meteorological, ecophysiological and soil science disciplines-to estimate forest transpiration, evaporation and evapotranspiration are compared. These include eddy covariance and scaled-up sap flow measurements, as well as two very different modelling approaches, i.e. a soil-related model and a physiological process model. The objectives were: (i) to quantify water vapour exchange between a 70-year-old Scots pine ecosystem and the atmosphere by estimating the various component fluxes in the forest's water balance, (ii) to compare multiple approaches to estimate water fluxes, and (iii) to identify and evaluate the strengths and short-comings associated with each approach.

2. Materials and methods

2.1. Experimental site and stand description

This study is based on experiments conducted during 1997 and 1998 in an even-aged (70-year-old), 150-ha mixed coniferous/deciduous forest-De Inslag-in Brasschaat ($51°18'33''$N, $4°31'14''$E), in the Belgian Campine region. The area surrounding the study site is urban (north and west) and rural, partially forested (south and east). The study stand is part of the European CARBO-EUROFLUX network and is a level II observation plot of the European programme for intensive monitoring of forest ecosystems (EC regulation No 3528/86), managed by the Institute for Forestry and Game Management (Flanders, Belgium). Mean annual long-term temperature at the site is 9.8 °C, with mean temperatures of the coldest and warmest months, 3 and 18 °C. Mean annual precipitation is 767 mm and is not seasonal. Apart from some small-scale terrain undulations of less than 1 m (trenches and mounds), the study site is flat (0.3% slope), and at 16 m elevation.

The forest consists of various patches with a wide variety in species composition and structure (de Pury and Ceulemans, 1997) (Fig. 1). The dominant overstory tree species are Scots pine (*Pinus*

Fig. 1. Map of the studied area: a 150-ha even-aged (70-year-old) mixed coniferous/deciduous forest in the Belgian Campine region, Northern Belgium ▨ deciduous, ▤ coniferous, ◩ mixed, ⠿ grassland, ● measuring tower.

sylvestris L) and pedunculate oak (*Quercus robur* L.). In 46% of the area the understory consists of various trees and shrubs (mainly *Prunus serotina* Ehrh. and *Rhododendron ponticum* L.), in 18% there is an understory of grass (*Molinia caerulea* (L.) Moench), and in 36% no undergrowth is present. The forest stand is equipped with a 39 m meteorological tower situated within the now 72-year-old Scots pine stand. In the vicinity of the tower no undergrowth is present as all understory has been removed three years before the study period. Average tree height is 21 m with a 3.7 m-canopy depth in this stand (Cermák et al., 1998). The stand has an open canopy with a 35% gap fraction (Van Den Berge et al., 1992) and a tree density of 560 trees ha^{-1}.

The upper soil layer ranges from 1.2 m to over 3 m in depth and has been described as a moderately wet sandy soil with a distinct humus and/or iron B-horizon; texture varies from sand to loamy sand (Meiresonne and Overloop, 1999). The soil type has been classified as a Psammentic Haplumbrept (U.S.D.A. classification) or a Umbric Regosol (F.A.O. classification) (Van Slycken et al., 1997). The soil was ploughed to a depth of 50–60 cm prior to the establishment of the forest in 1929. The topsoil lies on a substrate of Campine clay of the interglacial Pleistocene (Tiglian) at variable depth.

Because of its coarse texture, the topsoil has a high hydraulic conductivity and is rarely saturated, but due to the presence of a clay layer, the site is poorly drained. Spatial heterogeneity in the position of the underlying clay layer and in topsoil texture significantly influence the depth of the water table and water availability. More detailed information on the soil and on local climatic conditions can be found in Roskams et al. (1997), Janssens et al. (1999) and Kowalski et al. (1999).

2.2. Description of the models

2.2.1. WAVE model: simulation of the water balance

The soil water model Water and Agrochemicals in soil, crop and Vadose Environment (WAVE) (Vanclooster et al., 1994) describes the transport and transformations of matter and energy in the soil, crop and vadose environment. Although the water transport module of WAVE was originally developed for agricultural crops, it has also been calibrated and validated for forest conditions (Hubrechts et al., 1997; Meiresonne et al., 1999; Verstraeten et al., 2001). This model describes one-dimensional soil water transport based on the soil hydraulic properties, according Richards (1931). These include soil moisture retention, using a power function model (van Genuchten, 1980) Eq. (2.2.1.1), and hydraulic conductivity (Gardner, 1958) Eq. (2.2.1.2).

$$\theta_h = \theta_r + \frac{\theta_s - \theta_r}{(1 + (\alpha|h|)^n)^m} \tag{2.2.1.1}$$

where θ_h is the volumetric soil water content at pressure head h ($m^3\ m^{-3}$), θ_s the saturated volumetric soil water content ($m^3\ m^{-3}$), θ_r the residual volumetric soil water content ($m^3\ m^{-3}$), α is the inverse of the air entry value (m^{-1}), n and m are shape parameters.

$$K(h) = K_{sat} \frac{1}{(1 + (Bh)^N)} \tag{2.2.1.2}$$

where $K(h)$ is the hydraulic conductivity at pressure head h ($cm\ day^{-1}$), K_{sat} the saturated hydraulic conductivity ($cm\ day^{-1}$), B and N are shape parameters.

The values of the parameters are listed in Table 1.

The soil profile is divided into a number of compartments of 50 mm thickness, and the total time period into discrete time increments of unequal lengths (time steps smaller than one day), for the numerical calculation of the soil water fluxes. The conductivity and the differential moisture capacity are linearised.

The potential stand evapotranspiration (ET_{pot}) is calculated by multiplying the potential evapotranspiration of a reference surface (ET_0) with a crop coefficient K_c. The reference surface is short cut grass with roughness length 0.0015 m, zero plane displacement 0.08 m and canopy resistance 70 s m^{-1}. ET_0 is calculated according to the Penman–Monteith equation (Monteith, 1965). For these calculations the meteorological data measured on top of the tower are used (39 m above ground, 18 m above forest canopy). Wind speed and vapour pressure deficit could be influenced by the canopy cover, but comparison of the obtained ET_0 values with those of a standard weather station at 37 km distance, revealed no significant difference. As there are no crop coefficient values available in literature for forest stands, K_c is obtained by dividing the monthly means of the potential evapotranspiration of coniferous forest by those of grass. These were calculated by Gellens-Meulenberghs and Gellens (1992) with data from a standard weather station at about 40 km from the experimental site, using a twenty year reference period (1967–1986). The K_c values used in this study are listed in Table 2.

The potential transpiration (T_{pot}) and evaporation (E_{pot}) are obtained by splitting ET_{pot} using the leaf area index (L) as splitting factor.

$$E_{pot} = e^{-0.6\ L\ ET_{pot}} \tag{2.2.1.3}$$

$$T_{pot} = ET_{pot} - E_{pot} - E_i \tag{2.2.1.4}$$

E_i is the interception and is calculated as the minimum of precipitation and interception capacity. The interception capacity is determined by the method of Leyton et al. (1967). For a number of showers, gross precipitation measured on top of the tower is plotted against the net precipitation. Ignoring gross precipitation values of less than 2.5 mm canopy interception capacity is estimated from a line drawn through these

Table 1
Parameters of the soil moisture retention curve and the hydraulic conductivity model for the whole profile of the 70-year-old Scots pine (*Pinus sylvestris* L.) stand in the Campine region, Northern Belgium

Depth (cm)	θ_r	θ_s	α	n	m	K_{sat}	B	N
0–40	0.045	0.40	0.0177	0.98	1	215	0.283	2.034
40–55	0.049	0.40	0.0144	1.57	1	11	0.023	2.717
55–125	0.049	0.40	0.0140	2.00	1	17	0.032	4.039
>125	0.250	0.48	0.0024	0.71	1	2	0.043	1.329

θ_s is the saturated volumetric soil water content ($m^3\ m^{-3}$), θ_r the residual volumetric soil water content ($m^3\ m^{-3}$), α is the inverse of the air entry value (m^{-1}), K_{sat} the saturated hydraulic conductivity ($cm\ day^{-1}$), n, m, B and N shape parameters.

Table 2
Monthly values of the crop coefficient K_c for a coniferous stand, based on data from a weather station at about 40 km from the experimental site

	January	February	March	April	May	June	July	August	September	October	November	December
K_c	1.09	1.12	1.15	1.14	1.13	1.14	1.16	1.16	1.15	1.18	1.17	1.07

points of maximum net rainfall. Extrapolated back to zero net precipitation, the intercept with the X-axis (gross precipitation) is a measure of the interception capacity and was estimated 1.9 mm in the experimental plot. Transpiration is calculated as the integral of root water uptake over the entire profile.

For each compartment, the root water uptake is calculated by multiplying the maximal root water uptake (S_{max}) with a sink term $\alpha(h)$ ($0 < \alpha(h) < 1$), which is based on the critical soil water pressure heads (h). S_{max} was highest in the top layer and the maximal total water uptake per day by the roots reached 2.8 mm over the first 20 cm. S_{max} diminished very quickly with depth so that the total water uptake under optimal conditions reached a total level of 3 mm day^{-1} over the entire profile. Water uptake is reduced at high-pressure head associated with anaerobiosis (near saturation) and becomes optimally at $h = 10$ cm. At a low evaporative demand roots can no longer extract water optimally at $h = 1000$ cm, and at a high evaporative demand at $h = 20$ cm. Roots cease water uptake at low pressures ($h = 1600$ cm) due to soil moisture stress. In the case of the pine forest stand, the presence of a groundwater table determined the bottom boundary condition. The ground water table was during the dry year of 1997 and the first part of 1998 rather low (1.3–1.7 m). Due to high rainfall in September 1998 the ground water table rose up to 30 cm. The model was calibrated by comparing the modelled and the simulated soil moisture profile of 1997. Mainly the maximal root water uptake and the sink terms were subject to calibration. S_{max} was based on the pattern of the root mass density of fine roots (<1 mm) as a function of depth (Janssens et al., 1999). Critical pressure heads were derived from literature (Vanclooster et al., 1994; Item 1978).

The WAVE model requires daily climate data as precipitation, reference potential evapotranspiration and interception capacity. The model produces daily and cumulative values of soil evaporation ($E_{s,W}$),

evaporated interception ($E_{i,W}$), transpiration (T_W) and evapotranspiration (ET_W). Additional outputs include the integrated upward and downward water fluxes, changes in water storage at the bottom of the profile and at the bottom of any selected compartment, and the moisture content and the soil water pressure head (and root water extraction) for each soil layer.

2.2.2. Process-based SECRETS model (all mathematical equations can be found in Appendix A)

The process model SECRETS is a sequential, multi-species and multi-structure simulator (Sampson and Ceulemans, 1999; Sampson et al., 2001). It simulates stand scale carbon and water fluxes using established process algorithms adapted from several sources. Namely, the model uses maintenance respiration and water balance formulations adapted from BIOMASS (McMurtrie and Landsberg, 1992), with photosynthesis modelled using the Farquhar formulation found in the sun/shade model (de Pury and Farquhar, 1997). Soil carbon (C) and nitrogen (N) pools and fluxes were coded from the GRASSLANDS DYNAMICS surface and soil sub-model (Thornley, 1998). Soil water holding capacity is calculated from the soil sand and clay fractions following Saxton et al. (1986). The model simulates on a daily time step, except for photosynthesis that runs on an hourly time step. Meteorological inputs to the model, measured on the site (see under Section 2.3.1), include daily incident short-wave radiation, daily maximum temperature, daily minimum temperature, daily maximum relative humidity, daily minimum relative humidity, average relative humidity, and precipitation. A detailed description of the mathematical equations and functions of SECRETS, as well as the list of parameters used in the present application, can be found in Appendix A, but a synoptic description of the strategy and concepts of the model are given below.

Evapotranspiration in SECRETS includes transpiration, canopy interception of precipitation, surface

litter interception, and soil evaporation. Interception of precipitation by the canopy includes foliage and stems (tree boles) interception. All of these water flux components are driven, or influenced, by Penman–Monteith heat transfer biophysics.

Transpiration in SECRETS (T_S) is determined by incident radiation (using Penman–Monteith) and leaf stomatal conductance to water vapor (g_s) (empirically estimated from photosynthesis). There are a series of equations used in the Penman–Monteith approach to calculate T_S.

The heat transfer equations used in the Penman–Monteith approach depend, in part, on canopy conductance to estimate the imposed rate of transpiration. Canopy conductance is derived from g_s and leaf area index (LAI). The Ball and Berry approach (Ball et al., 1987) is used as adapted by Leuning (1995) to estimate g_s from hourly photosynthesis. Canopy conductance (G_C, mol m^{-2} ground s^{-1}), then, is integrated over the canopy as:

$$G_C = \int g_s dL \qquad (2.2.2.1)$$

where L is LAI (m^2 m^{-2}; projected area basis). LAI is a daily input into the model and was estimated for this site using the LI-Cor LAI-2000 Plant Canopy Analyzer (as detailed further). The instantaneous rate of canopy transpiration ($T_S(t)$; mm h^{-1}) depends on the equilibrium rate of transpiration, the imposed rate of transpiration, and the extent to that transpiration is determined by incident radiation versus canopy conductance (Jarvis, 1985). The coupling coefficient (Ω) describes the extent to which $T_S(t)$ depends net radiation K_n (MJm^{-2}d^{-1}) versus G_C and is estimated as:

$$\Omega = (s + \gamma)/s + \gamma + \gamma(G_b/G_C) \qquad (2.2.2.2)$$

where G_b is canopy boundary layer conductance (mol m^{-2} s^{-1}), s is the slope of saturation vapour-pressure/temprature curve and γ the psychrometric coefficient (pa°c^{-1}) (see Table A1).

The instantaneous rate (mm h^{-1}) of canopy transpiration ($T_S(t)$) is calculated as:

$$T_S(t) = T_{Seq}\Omega + T_{Simp}(1 - \Omega) \qquad (2.2.2.3)$$

where: T_{Seq} = equilibrium rate of transpiration (see Appendix A)

T_{Simp} = imposed rate of transpiration (see Appendix A)

Finally, daily transpiration (mm day^{-1}) is calculated as:

$$T_S = f_E \int T_S(t)dt \qquad (2.2.2.4)$$

where f_E is the reduction of transpiration when canopy is partially wet.

Canopy interception in SECRETS is determined by LAI, average tree diameter at breast height, and incident radiation. For days with precipitation events, the interception of precipitation by foliage is calculated as the minimum estimate between that derived empirically, and that estimated from Penman–Monteith, as shown in Appendix A. As mentioned, the model also uses an empirical estimate of the amount of precipitation intercepted by individual tree boles. This equation was adapted from Loustau et al. (1992a) and is defined as:

$$\text{Stem Flow} = \text{Precip} \times B \times \text{dbh} \qquad (2.2.2.5)$$

where Precip is the precipitation (mm d^{-1}), B the empirical coefficient (1/m), dbh is the diameter at breast height (m).

The total amount of daily precipitation (for precipitation events) intercepted, then, is the summation of that intercepted by foliage and stems.

Evaporation of precipitation from the surface litter (mm day^{-1}) is derived in a similar way as that from the wet foliated canopy. Evaporation of water from the soil profile depends on the Penman–Monteith equations described above with obvious changes in the input parameters. Namely, dependencies of Ω use soil aerodynamic conductance (G_S) and soil diffusive conductance (G_d) instead of the comparable canopy parameters. In a similar fashion, the imposed rate of evaporation also depends on G_d.

Parameters and parameter estimates used in the equations discussed above may be found in Table A1.

2.3. Measurements

2.3.1. Supporting measurements

Climatological parameters, i.e. global radiation (Kipp and Zonen CM6B, the Netherlands), incoming photosynthetically active radiation (PAR; 400–700 nm; JYP-1000 sensor, SDEC, Tours, France),

temperature and relative humidity (Didcot Instrument Co Ltd, Abingdon, United Kingdom DTS-5A), windspeed (Didcot DWR-205G) and precipitation (Didcot DRG-51) are continuously measured and recorded half-hourly at the top of the tower. An ultrasonic anemometer (Gill Instruments Solent Research, UK) measured 3D windspeed (Overloop and Meiresonne, 1999).

Soil moisture content was measured twice a week with two series of TDR-sensors (Time Domain Reflectometry), placed every 25 cm down to a depth of 175 cm (cabeltester: Tektronix 1502B, Redmond, USA). The net precipitation was determined by measuring the throughfall collected by 6 m^2 of gutter by a flowmeter (Didcot DFM-250), and the stemflow collected by spirals along 4 representative trees. Data on net precipitation are available for only a limited time period (second half 1998). Water table fluctuations were recorded continuously down to a depth of 2.2 m by a pressure sensor (Didcot DWL-10) (Meiresonne and Overloop, 1999). LAI was measured on eight days during the year with a pair of light sensing instruments (LAI-2000, Li-Cor Inc., Lincoln, NE, USA) (Gond et al., 1999). The LAI-2000 measures half of the total surface leaf area and necessary corrections were made according to Stenberg (1996). LAI changed significantly during the growing season and values ranged from 1.7 to 3.0. These values were used in the consequent modelling exercises.

2.3.2. Eddy covariance flux measurements

The eddy covariance system is described by Kowalski et al. (1999). Turbulent fluctuations were measured at 41 m above the ground with a 3D sonic anemometer (winds and 'sonic' temperature) and an infrared gas analyser (CO_2 and H_2O gas concentrations; LiCor LI-6262, Inc. USA). The EDISOL program (Moncrieff et al., 1997) logged data and calculated fluxes in real time. Turbulent fluxes were defined as half-hour means of deviations from an approximation to a 200-s running mean filter, utilising three-dimensional co-ordinate rotations as described by McMillen (1988). This is the standard EURO-FLUX methodology (Aubinet et al., 2000). The eddy flux data have gaps of several weeks due to equipment failure during May 1997 (pump), September 1997 (gas analyser), May 1998 (anemometer electronics)

and December 1998 (gas analyser). Half-hour periods with raw data that failed statistical quality control (Vickers and Mahrt, 1997) were removed from the data set, introducing more gaps.

The eddy correlation instruments measure atmospheric fluxes directly. However, linking these fluxes to ecosystem exchange depends on numerous assumptions. To facilitate a simple interpretation, many atmospheric processes that can affect the fluxes are ignored. These include phase change (e.g. evaporation of rain or fog, and fog formation), moisture advection (such as in frontal passage), and mixing against local gradients associated with terrain outside the forest. Ecosystem water vapour exchange is estimated from half-hour covariance's assuming the existence of a well-defined spectral gap between the synoptic flow and turbulent motions (Galmarini and Thunis, 1999). The turbulence is assumed to be homogeneous and stationary, based on flow over a flat and homogeneous upwind surface. Finally, surface exchange processes under consideration exclude formation and evaporation of dew at the canopy and litter surfaces.

The measured eddy fluxes are thus interpreted as representing total forest evapotranspiration (ET$_{EC}$). Because rainfall greatly influences the reliability of the eddy flux data, the correlation between the models and the eddy flux has only been examined on days without precipitation.

2.3.3. Measurement of sap flow rates

2.3.3.1. Theory and methodology. The sap flow was measured by the heat field deformation (HFD) method (Nadezhdina et al., 1998). Briefly, the method is based on the observed changes of artificial heat field around the linear heater in stems depending on the sap flow rate and xylem tissue properties (Nadezhdina and Cermák, 1999). The heat field is almost circular around a linear heater inserted in the xylem along stem radius under zero flow, but is getting asymmetrical (prolonged in axial direction and shortened in tangential direction) under conditions of usual flow rates as verified in situ using the network of miniature thermometers (Nadezhdina, 1999) and the infra-red camera (Nadezhdina et al., 2000). The main points of the heat field were characterised by temperature differences, measured by a series of thermocouples inserted in the stem at

the axial direction (up and down the heater, dT_{sym}) and at the tangential direction (on the sides of the heater, dT_{asym}). Such input data are basically related to calculate the sap flow as:

$$Q_w = (dT_{sym}/dT_{asym}) \times F_{geom} \times F_{matrix} \qquad (2.3.3.1)$$

where F_{geom} and F_{matrix} are terms including sensor geometry and matrix properties, described by a number of additional equations (Nadezhdina and Cermák, 1999).

The new combined sensor (Nadezhdina et al., 1998; Nadezhdina and Cermák, 1999) applies two pairs of thermocouples situated in the stem around the linear needle-like (linear) heater. One pair of thermocouples is installed symmetrically with both ends in axial direction up and down the heater (it measures the temperature difference dT_{sym}) and another pair is installed asymmetrically on the side of the heater with the reference end at the same height as the reference end of symmetrical pair of thermocouples (it measures the temperature difference dT_{as}). Two asymmetrical thermocouples on both sides of the heater could be used to get better averaging of flow over twice as much wide directly measured stem segment. All thermocouples and the heater are placed in stainless steel hypodermic needles (1.2 mm in outer diameter). When using a sensor for measurement of the radial pattern of sap flow, two pairs of long needles with series of thermocouples in each of them arranged at different distances (from 5 to 15 mm) are applied. Heating power P is rather low, usually below 0.1 W per unit length (1 cm) of the heater.

Data of temperature gradients near the heater were used to characterise the shape of the heat field around the heater. Changes in the shape of such heat field under different sap flow rates are measured by the set of thermocouples situated at different distances in axial and tangential directions. The shape of heat field changes significantly with increasing and/or decreasing sap flow, when different amount of heat is moved axially along tree axis and at the same time tangentially towards both sides of the heater. The shape of heat field in addition to sap flow depends on wood structure, density, water content and wood thermodynamic properties determined by the above parameters.

Changes of heat field around the heater due to moving sap and varying properties of

the conductive system can be presented using the ratio of temperature differences dT_{sym} and dT_{as}:

$$dT_{sym} = T_u - T_d \qquad (2.3.3.2)$$

$$dT_{as} = T_m - T_d \qquad (2.3.3.3)$$

where T_u, T_m, T_d are temperatures of the upper, middle and lower thermometers (i.e. ends of thermocouples), respectively. Experimentally it was confirmed, that the ratio of both the above mentioned temperature differences (dT_{sym}/dT_{as}) is proportional to sap flow rate:

$$Q_w = K_p \frac{dT_{sym}}{dT_{as}} \qquad (2.3.3.4)$$

where k_p is a physical constant, including basically geometry of the measuring point and physical properties of the conductive system.

$$K_p = f(\text{geom}; k_{st}; c_w) \qquad (2.3.3.5)$$

where k_{st} is heat conductivity of stem and c_w is specific heat of water.

Because of the asymmetrical pair of thermocouples in the HFD sensor, dT_{as} is not sensitive under very low flows (similarly like in the THB and similar sensors). Thanks to the practically constant value of dT_{as}, the dT_{sym} can be involved alone in this range of flows, where it is very sensitive to flows in both directions. Therefore the HFD sensor can indicate zero flow but also reversed flow (e.g. at night after long rain or during fog), providing that such flow is low.

2.3.3.2. Validiation of the methodology. The approach and methodology outlined above have already been extensively validated in the field at the tree level: (1) through comparison with volumetric measurements on several lime trees, (2) through comparison with the heat balance method (Nadezhdina and Cermák, 1999) and (3) during various root to branch communication experiments (Nadezhdina and Nadezhdin, 2001). At the stand level, the results of the HFD method (stand transpiration estimates based on series of measured sample trees) were validated in contrasting (wet and dry) forest stands: (1) by comparing with results obtained by the micro-meteorological method and (2) using models which applied remote sensing data (Chiesi et al., 2002).

2.3.3.3. Scaling-up to tree and stand levels. The up-scaling of the sap flow to the whole tree level as well as an analysis of the possible errors that could arise during the flow integration or up-scaling procedure from single-point measurements to whole trees have already been described (Nadezhdina et al., 2002). The up-scaling of data from a series of sample trees to the stand level was done on the basis of selection of representative size of sample trees using quantils of total and using forest inventory data (basal area) as a biometric background (Cermák and Kucera, 1987, 1990; Cermák and Michalek, 1991).

2.3.3.4. Uncertainty analysis. Uncertainties are usually associated with fundamental methodological problems of sap flow, with natural variation at different levels of biological organisation, and with the uncertainties involved in up-scaling. In summary the uncertainties can be described as follows.

Methodological and integration problems of different sap flow methods were reviewed by Lundblad et al. (2001) and Kostner et al. (1998). Additional errors could be associated with the possible non-parallelism of inserted needles, individual differences in xylem heat conductivity in axial and tangential directions, temporal variations, etc.

Variation at the tree level includes (1) non-uniformity of sap flow along the radius. This is most important and may cause problems when the radial pattern of the flow is neglected (as is done in most studies); (2) determination of the sapwood depth; (3) the positioning of sensors beneath the cambium; (4) variation of the sap flow around the stem, etc.

Variation at the stand level includes variation between trees (even trees of the same size) and the corresponding representative size and number of selected sample trees.

The up-scaling procedure from the tree to stand level depends on the application or selection of suitable biometric variables.

Terms and abbreviations used in this comparative study are provided in Table 3.

2.4. Inventory of data availability

Each approach examined in this study had a separate temporal scale in the resolution of the water

Table 3
Overview/summary of the output and the symbols of the four different approaches for the quantification of the evapotranspiration used in this study

Technique/ method	Output	Symbol
WAVE: water balance model	Transpiration	T_W
	Evaporation of intercepted water	$E_{i,W}$
	Soil evaporation	$E_{s,W}$
	Evapotranspiration $= T + E_i + E_s$	ET_W
SECRETS: process-based model	Transpiration	T_S
	Evaporation of intercepted water	$E_{i,S}$
	Soil evaporation (including litter evaporation $E_{l,S}$)	$E_{s,S}$
	Evapotranspiration $= T + E_i + E_s$	ET_S
Eddy covariance flux measurement	Evapotranspiration	ET_{EC}
Sap flow measurement	Transpiration	T_{SF}

flux estimates and two of the four approaches took place during different periods. Accordingly, not all cross-method comparisons at the measurement, or simulation, scale examined were available (or warranted). In this study two years are considered: 1997

Table 4
Availability (period) of the experimental or simulated data (transpiration, interception evaporation, soil evaporation and evapotranspiration) and resolution of the fluxes for the 70-year-old Scots pine (*Pinus sylvestris* L.) stand in the Campine region, Northern Belgium, used in this study

Technique/ method	Period	Flux resolution	N
WAVE: water balance model	1/1/97–31/12/98	Daily	730
SECRETS: process-based model	1/1/97–31/12/98	Daily	730
Eddy covariance flux measurement	1/1/97–31/12/98	Half hourly	223
Sap flow measurement	15/7/97–31/8/97	15 min	49

N is the number of days with reliable data.

and 1998. Table 4 provides a summary of the measurement and simulation periods examined, and the time scale associated with each approach. Sap flow measurements were made continuously from 15 July to 31 August during 1997. The eddy covariance measurements were available throughout 1997 and 1998, however data gaps were common due to instrumentation and software problems. The sap flow and the eddy covariance measurements had a similar time measurement basis; measurements were done on a half-hourly basis.

3. Results

3.1. Meteorological conditions during this study

Despite similarities in mean annual temperature, 1997 and 1998 had substantially different meteorological conditions. In 1997 Belgium experienced continental (as opposed to the typical maritime conditions) conditions, including a very cold, dry January and a hot August compared to 1998 (Table 5). There was considerably more sunshine in 1997 and annual precipitation (672 mm) was only 88% of the long-term mean. In contrast, precipitation in 1998 exceeded local rainfall records (1042 mm were recorded in Brasschaat), particularly extreme during autumn (September: 280 mm, October: 139 mm, and November: 118 mm).

Table 5
Meteorological conditions during the two research years of this study, 1997 and 1998, at the 70-year-old Scots pine (*Pinus sylvestris* L.) stand in the Campine region, Northern Belgium. Temperatures shown are the means of average daily atmospheric temperatures

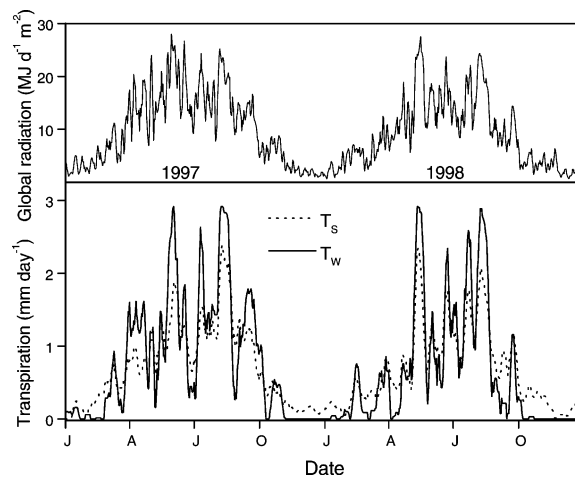| Meteorological parameters	Unit	1997	1998
Mean annual temperature	°C	10.4	10.7
Mean temperature of coldest month	°C	−0.7	4.1
Mean temperature of warmest month	°C	20.6	17.3
Annual precipitation	mm	672	1042
Mean daily incoming radiation sum	MJ m^{-2} day^{-1}	10.17	8.89

Fig. 2. Incident global radiation (top panel) and seven day running mean of transpiration simulated by the models WAVE (T_W; solid line) and SECRETS (T_S; dashed line) (lower panel) in a 70-year-old Scots pine (*Pinus sylvestris* L.) stand in the Campine region, Northern Belgium for 2 consecutive years (1997, 1998).

3.2. Transpiration

Both models (WAVE and SECRETS) exhibited similar seasonal trends in simulated transpiration that corresponded to incident global radiation. However broad separation between the two was apparent during markedly low and high incident global radiation (Fig. 2). During this weeks WAVE simulated an increased amplitude in transpiration (T_W) and a corresponding increased departure from the transpiration simulated by SECRETS (T_S). In addition, WAVE estimated very little to no T_W during late autumn, winter and early spring when SECRETS simulated slight (0.1–0.5 mm day^{-1}) T_S fluxes (Fig. 2). The direct correlation between simulated transpiration and global radiation for the models indicated a lower coupling for WAVE with asymptotic responses for low and high radiation periods (Fig. 3). Overall, this resulted in a lower total annual T_S estimate for SECRETS (18%) in 1997, but a slightly overestimate in 1998 (5%) (Table 6) when compared to WAVE (T_W).

At first view the global pattern of the transpiration simulated with the models (T_W and T_S) and those estimated from sap flow shows similarity (T_{SF}) during the 1997 period comparison (Fig. 4). In fact, SECRETS fits very well, with maximum differences
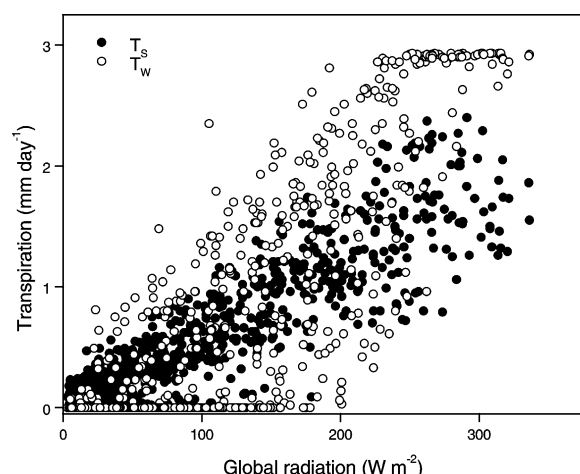
Fig. 3. Daily total transpiration simulated by the models WAVE (T_W; open circles) and SECRETS (T_S; black circles) versus global radiation in a 70-year-old Scots pine (*Pinus sylvestris* L.) stand in the Campine region, Northern Belgium for 1997 and 1998.

in T_S of 0.4–0.5 mm day^{-1} when compared to the sap flow measurements, but more commonly within 0.1–0.3 mm day^{-1}. Simulated T_W from WAVE was consistently lower than T_S from SECRETS and T_{SF} measured from sap flow during days of precipitation events, and higher (up to 58%) when rain was absent

Table 6
Precipitation values (mm) and simulated components of the evapotranspiration (mm) of the 70-year-old Scots pine (*Pinus sylvestris* L.) stand in the Campine region, Northern Belgium, during three different periods: complete year 1997, complete year 1998 and the period of the sap flow campaign (14/7/97–31/8/97)

Period		1/1/97–31/12/97	1/1/98–31/12/98	14/7/97–31/8/97
WAVE	Precipitation	672	1042	115
	$E_{s,W}$	206	200	50
	$E_{i,W}$	157	206	31
	T_W	295	226	83
	ET_W	658	632	164
SECRETS	$E_{s,S}$	211	219	35
	$E_{i,S}$	113	162	21
	T_S	243	238	69
	ET_S	567	619	125
Sap flow	T_{SF}	–	–	62

Results of the WAVE and SECRETS models, as well as the scaled-up sap flow have been presented. All values are in mm water. Symbols and abbreviations are as in Table 3.
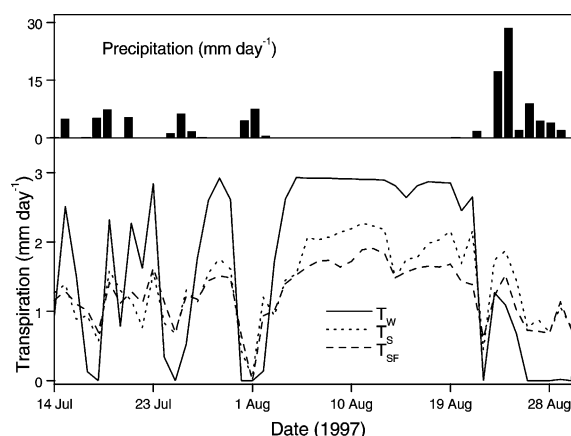

Fig. 4. Precipitation (upper panel) and daily totals of transpiration (lower panel) of a 70-year-old Scots pine (*Pinus sylvestris* L.) stand in the Campine region, Northern Belgium during the sap flow measurement campaign of 14 July to 31 August 1997. Transpiration estimates by the sap flow method (T_{SF}; dashed line), the WAVE model (T_W; solid line), and the SECRETS model (T_S; pointed line) are being presented.

(Fig. 4). For the relationship between simulated transpiration T_w and measured transpiration T_{SF}, a linear model is not appropriate, however a sigmoïdal course is observed (Fig. 5). For $T_W = 0.0$ mm day^{-1}, T_{SF} varies between 0.0 and 1.2 mm day^{-1}. From T_W 0.1 to 2.0 mm day^{-1} there is nearly no change in
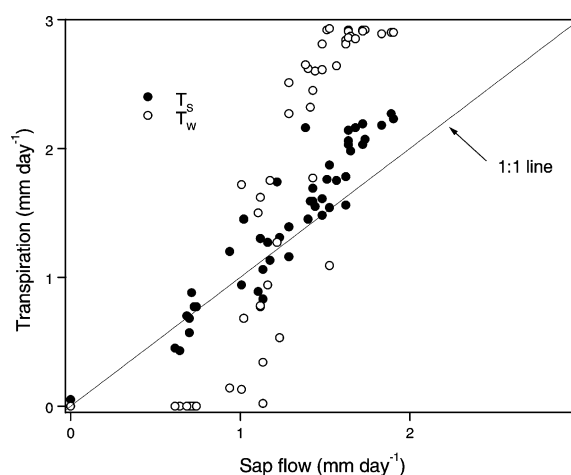

Fig. 5. Simulated daily totals of transpiration of a 70-year-old Scots pine (*Pinus sylvestris* L.) stand in the Campine region, Northern Belgium, by the models WAVE (T_W; open circles) and SECRETS (T_S; black circles) versus transpiration estimated by the sap flow method (T_{SF}) during the sap flow measurement campaign of 14 July to 31 August 1997.

the average T_{SF} but with a large variation around the mean. Then from T_W 2.0 to 3.0 mm day^{-1} there is a very steep slope up to a horizontal asymptote at $T_W = 3.0$ mm day^{-1}. The SECRETS model performs much better than the WAVE model. This visual assessment is confirmed by a more formal (linear) regression analysis. This regression has R^2 of 0.874 with standard error (noise around the regression line) of 0.204. The slope is 1.31 with standard error of 0.0725. However, when integrated over the summer of 1997, both models over-estimated transpiration ($T_S = 69$ mm [11%], $T_W = 83$ mm [34%]) when compared to the empirical estimates ($T_{SF} = 62$ mm).

3.3. Evaporation

3.3.1. Interception evaporation (E_i)

As expected, increased precipitation resulted in increased canopy evaporation (E_i) in the model comparisons (Fig. 6). Both models had a clearly delineated threshold response to precipitation when rainfall was less than 4 mm day^{-1}; both models exhibited a similar slope when simulated daily E_i was one mm or less (Fig. 6). However, whereas WAVE ($E_{i,W}$) reached an asymptote at 1.9 mm day^{-1} (potential interception capacity of the canopy),

estimates from SECRETS ($E_{i,S}$) diverged at about 1 mm day^{-1}. This corresponded to a reduced trajectory in simulated $E_{i,S}$ with increased precipitation for SECRETS (Fig. 6). The reduced slope resulted in higher daily estimates of $E_{i,W}$ from WAVE when precipitation was less than about 10 mm day^{-1}. This was reflected in the annual estimates of E_i, with WAVE simulating 39% greater interception in 1997 and 27% greater in 1998 (Table 6). There was a preponderance of days at or near maximum interception for both models.

3.3.2. Soil evaporation (E_s)

Annual estimates of soil evaporation are, conversely, very similar between the two models. Annual $E_{s,S}$ simulated by SECRETS was only marginally (2%) higher than that simulated by WAVE ($E_{s,W}$) in 1997 and only 10% higher in 1998 (Table 6). However, similarity in the annual estimates did not correspond to similarity in the direct comparison of daily values between the two models (Fig. 7). Although there was reasonable correlation in simulated soil evaporation between WAVE and
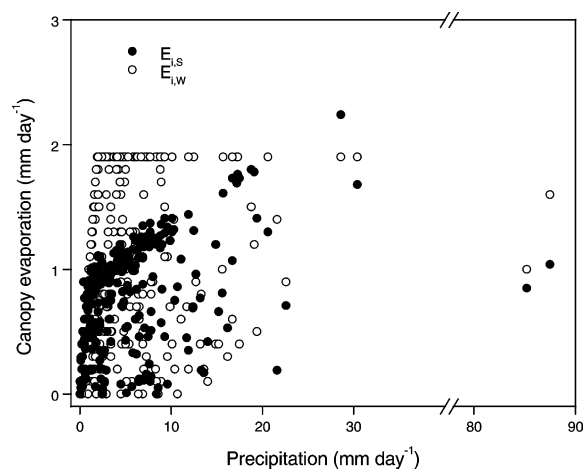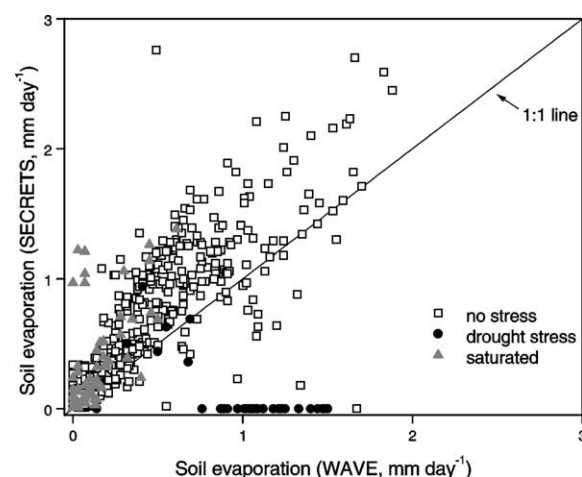
Fig. 6. Daily totals of canopy evaporation simulated by the WAVE model ($E_{i,W}$; open circles) and the SECRETS model ($E_{i,S}$; black circles), versus daily total precipitation in a 70-year-old Scots pine (*Pinus sylvestris* L.) stand in the Campine region, Northern Belgium for 1997 and 1998.

Fig. 7. Comparison of daily totals of soil evaporation simulated by the WAVE model ($E_{s,W}$) and the SECRETS model ($E_{s,S}$) in a 70-year-old Scots pine (*Pinus sylvestris* L.) stand in the Campine region, Northern Belgium for 1997 and 1998. Days with drought stress (soil water content (SWC) at 25 cm depth below 10 vol.%) are indicated by black circles, days without soil water stress (SWC between 12.5 and 20 vol.%) are indicated by open squares, days with saturated soil (SWC more than 25 vol.%) are indicated by grey triangles.
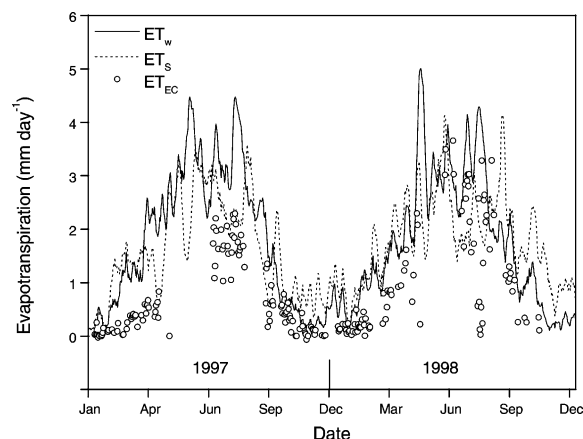
Fig. 8. Daily totals of the evapotranspiration (lower panel), measured by the eddy covariance technique (ET_{EC}; open circles) on dry days, and seven day running means of evapotranspiration as simulated by the models WAVE (ET_W; solid line) and SECRETS (ET_S; dashed line) in a 70-year-old Scots pine (*Pinus sylvestris* L.) stand in the Campine region, Northern Belgium for 2 consecutive years (1997, 1998).

3.4. Evapotranspiration

Seasonal trends in evapotranspiration (ET) of the two models are not consistent and were both poorly correlated with the eddy-covariance measurements (ET_{EC}) (Fig. 8). The models over-estimated ET throughout most of 1997 when compared to ET_{EC}, but did marginally better during the autumn of 1997 and during most of 1998.

Larger differences in simulated ET between the two models were apparent during low and high soil water content days (Fig. 9a and b). There is an impact of the SWC on the relation between measured and simulated ET. On low soil water content days (SWC $< = 10\%$) there is no relation between measured and simulated values with a insignificant slope of linear regression ($p = 0.1$ and 0.4 for, respectively, WAVE and SECRETS). In fact except for two points in the left bottom—the simulated values remain fluctuate around a constant. For the WAVE model the constant (the average) is 3.225 ± 0.212 standard error (s.e.) and for SECRETS 1.654 ± 0.094 (s.e.). Also R^2 is very low (0.1 and 0.03 for, respectively, WAVE and SECRETS). On days with high soil water content (SWC $> 10\%$) there is a relationship. For WAVE, except at very low values of the measured ET_{EC}, the moving regression line lies higher than the one for the SECRETS model.

SECRETS, this relationship was non-linear, with SECRETS often simulating greater $E_{s,S}$ throughout the comparison. Overall, higher daily estimates of $E_{s,S}$ were offset by many days of zero $E_{s,S}$, simulated by SECRETS. Zero values corresponded to days when volumetric soil water content dropped below about 10% (Fig. 7).
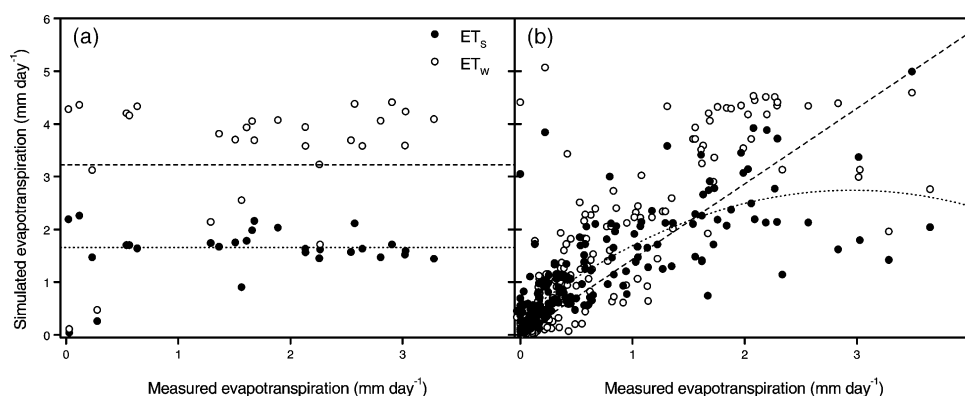

Fig. 9. Comparison between daily totals of evapotranspiration of a 70-year-old Scots pine (*Pinus sylvestris* L.) stand in the Campine region, Northern Belgium, as simulated by the models WAVE (ET_W; open circles) and SECRETS (ET_S; black circles) and as measured by the eddy covariance technique (ET_{EC}) on dry days during 1997 and 1998. (a) Presents data obtained on days with low soil water content (less then or equal to 10% at 25 cm depth); the dotted line represents the mean value estimated by WAVE and the dashed line represents the mean value estimated by SECRETS. (b) Presents data obtained on days with high soil water content (more then 10% at 25 cm depth); the dotted line represents the best linear fit for WAVE; the dashed line represents the best quadratic fit for SECRETS.

On average, for both the estimate of ET is higher than the measured value. For Secrets a quadratic model holds (the *p*-value for the third order term of the polynomial is 0.646, while for the second order term it is 0.000). This is an indication that the higher values of the measured ET_{EC} become again very similar to the simulated values of SECRETS. For the WAVE model a fairly good linear regression line fits. Only three outliners are present. The regression coefficient is 1.44 ± 0.079 (s.e.). This makes clear that the simulated ET_W is about a half higher than the measured ET_{EC}. Annual budgets for the ET_{EC} were not available due to data gaps, however both models were relatively similar in their annual ET estimates. Simulation results were 658 mm (1997) and 632 mm (1998) for ET_W of WAVE and 567 mm (1997) and 619 mm (1998) for ET_S for SECRETS.

4. Discussion

4.1. Four methods to assess (evapo)transpiration: strengths and weaknesses

There are many ways to estimate water vapour exchange in forest ecosystems. Cross-method comparisons highlight the strengths and weaknesses of often-disparate approaches and, in principal, provide clues as to where improvements can be made (Calder, 1977; Stewart, 1984; Wilson et al., 2001). The four methods examined in this study differed substantially in their formulation and approach. Essentially, these four methods spanned cellular to ecosystem scale resolution in their measurement inputs and in their process-level formulation of water flux outputs. Yet, overall, reasonably good agreement was found among several of the comparisons made when outputs were resolved at comparison-specific time scales. In particular, daily estimates of transpiration simulated by SECRETS were well correlated with those estimated by the sap flow technique. And, especially considering the diametrically opposed formulations between the WAVE and SECRETS models, daily estimates of transpiration and soil evaporation (data not shown) differed by up to 1.2 mm depending on the absolute flux. Moreover, the annual sums for transpiration and soil evaporation were very similar. Neither model performed very well when compared to

the eddy covariance approach. It should be mentioned that the SECRETS model had been fine tuned and calibrated for the experimental forest site using the carbon pools and fluxes (Sampson and Ceulemans, 1999; Sampson et al., 2001), but that no specific fine tuning or improved calibration was made with regard to the water fluxes.

Model behaviour can, beneath the parameterisation technique, be explained by the algorithms used to estimate the components of water flux and the driving forces considered. The WAVE model simulates the transpiration of trees on a ground area basis using point measurements of soil characteristics, soil water availability and water balance components (e.g. through-fall, rainfall). In WAVE, the soil substrate determines how the trees can meet the atmospheric demand of water (ET_0), with fine root biomass and rooting depth determining a threshold potential for water movement through, in this case, trees. The model is thus very specific in the soil characteristics determining simulated water fluxes; spatial variation in soil texture and soil physical properties are thus important in simulating water fluxes. In this formulation the soil itself drives water vapour exchange with the atmosphere, irrespective of the direct, instantaneous biological aspects pertaining to plant growth. Conversely, SECRETS is a mechanistic process model. Transpiration is estimated by imitating the biological process of water vapour exchange through stomata on individual leaf surfaces. In addition, canopy interception of water is determined by the LAI in conjunction with the energy required to evaporate water on the leaf surfaces, taking into account boundary layer resistance to water vapour exchange and leaf energy balance. In this formulation the plant system drives water exchange with the atmosphere.

Much of the variability in water fluxes between the models can be explained by the manner in which precipitation and global radiation impact flux estimates. The soil driven WAVE model responds to threshold changes in soil water inputs immediately following precipitation events. Canopy interception in WAVE is calculated as the minimum between precipitation and the potential interception capacity. This formulation can lead to some spurious results at low precipitation levels, especially when gaps are present in the forest canopy, as is the case in this

study. However, since evaporation of intercepted water reduces the amount of transpiration, a relatively large error in interception leads to only a relatively small error in the final calculation of evapotranspiration.

The sap flow method provides a direct estimate of the upward water movement inside individual trees in the stand. However, many assumptions are required in the up-scaling approach that introduces bias and error, in the half-hourly estimates. Sampling errors result from scaling-up processes that occur at small scales to larger spatial and temporal scales (Jarvis, 1995). In this case the transpiration estimates depend on a sub-sample of trees that is assumed representative of the population of trees within the stand. Errors can also occur if the radial patterns of sap flow in the tree trunks are not considered (Hatton et al., 1995; Cermák and Nadezhdina, 1998). In addition, up-scaling from the sample trees to the whole stand requires an accurate estimate of the distribution of suitable biometric parameters of the stand (Cermák and Kucera, 1990; Cermák 1989). Linear regression between the daily tree sap flow and the tree basal area, as used in this study, was also found by Martin et al. (2001) for a 220-year-old *Abies amabilis* forest. Systematic errors include instrument bias and those that result from the measuring system/physical environment interaction (Goulden et al., 1996). The estimate of the forest transpiration from sap flow measurements thus depends not only on the accuracy of the sap flow measurement, but also on the proper integration and up-scaling procedure used (Nadezhdina et al., 2001), and the stem frequency distribution (sapwood area) throughout the forest. Regardless, the sap flow approach to estimate forest transpiration has clear advantages. The approach is relatively simple, it is based on the sound biological premise that sapwood area (xylem wood) conducts water movement through trees, and the individual measurements needed in the up-scaling process be easily assessed. In addition, it can be easily applied for long-term studies in any terrain and climatic conditions (Cermák et al., 2001; Cermák and Kucera 1987; Cienciala et al., 1997; Jimenez et al., 1996). Comparing results of the sap flow approach to results of micro-meteorological methods and hydrological models confirm that it can be reliably applied in large-scale studies, however more often in the qualitative sense (Wilson et al., 2001).

The eddy covariance fluxes represent direct measurements of water fluxes that can be correlated to the total evapotranspiration of the entire forest (a mix of both pine and oak trees). However, based on energy balance calculations, eddy covariance measurements appear to underestimate forest-atmosphere exchange, typically by about 25% (Baldocchi and Vogel, 1996). Several possible explanations have been proposed for the apparent 'loss of flux' at the Brasschaat site, which approaches 30% (Ceulemans et al., 2002). The exclusion of motions on time-scales longer than 200 s necessarily eliminates large eddy transport; this could imply underestimation of canopy exchange, particularly during summer periods of high transpiration, when large convective motions are most likely. The EUROFLUX methodology (described in the material and methods) is adhered, because low-frequency fluxes are very difficult to isolate from the effects of atmospheric non-stationarity. In Brasschaat, the combination of a high tower and a small forest calls into question the adequacy of fetch at this site (100 m). This problem, however, may be less important during periods of high transpiration, and this is unlikely to be a large source of error in the estimates presented here. This question remains a subject of ongoing research. Finally, the closed-path system used in this study likely loses some of the high frequency eddy fluctuations due to tube mixing and filtration. In particular, accumulation of hydrophilic material at the sample inlet filter, which was changed weekly, provides a deliquescent water buffer, which may reduce the measured variations. Accumulation of rainwater at the inlet, and subsequent aspiration by the pump wets the filter; this is one reason why closed-path systems have difficulties during periods of precipitation. However, simple accumulation of particulate matter can also result in a wet filter. The correction of such effects by spectral techniques was examined and found to be small and highly uncertain, and therefore was abandoned.

4.2. Comparison with published observations

Similar comparisons between various methods to determine forest (evapo)transpiration as the one presented here, have been made, among others, on maritime pine in Portugal (Berbigier et al., 1996; Loustau et al., 1996), on beech in France (Granier et al., 2000), on Sitka spruce in Scotland

(Milne et al., 1985), on mixed deciduous forest in the South-eastern United States (Wilson et al., 2001). Measured and modelled stand transpiration were in good agreement in the beech study (Granier et al., 2001) and Berbigier et al. (1996) reported that also the comparison between estimations of canopy evaporation by eddy covariances and sap flow was satisfactory in maritime pine. Qualitative similarities between sap flow and eddy covariance estimates on a daily basis were found in the mixed deciduous forest (Wilson et al., 2001). However, none of the comparisons reported in literature showed perfect agreement.

Comparable estimates of transpiration and evapotranspiration from the literature for Scots pine stands of similar structure, climate, and growing season are few, with those from the United Kingdom and Germany most applicable. The results of the present study were consistent with regional simulations for Scots pine stands across Europe over a latitudinal range of over 20° (Berninger, 1997). A stand of similar latitude and LAI, but lower average temperature (8.7 °C) in Germany had nearly identical year-end estimates of transpiration (~ 250 mm yr^{-1}) (Berninger, 1997) as that simulated with SECRETS for both years and with WAVE for 1998, but slightly lower than that estimated by WAVE for 1997 (Table 6). Our yearly estimates from both models lie within the regional average simulated by Berninger (1997). Transpiration of a more northerly stand in Scotland with similar LAI and stocking reached 2 mm day^{-1}, exhibiting a similar seasonal depression during summer as that found in Brasschaat (Irvine et al., 1998). Their estimates were slightly lower than those simulated in this study (Fig. 2), but closer to that found in the scaling-up approach (Fig. 4). However, they observed a higher than usual hydraulic resistance in their study which reduced transpiration, and average temperatures (and most likely incident radiation) at their site were somewhat lower (Irvine et al., 1998).

Several studies permitted a comparison of evapotranspiration. Waring et al. (1979), in a scaling-up exercise, found close coupling between sapwood water deficit and ET for Scots pine stands in North-eastern Scotland. There, evapotranspiration varied from about 0.5–4 mm day^{-1}, with ET exceeding 6 mm day^{-1} at one occasion. Present estimates of ET

varied over a similar range, however those from WAVE (ET$_W$) were, on occasion, 30% higher than SECRETS and those found by Waring et al. (1979) (Fig. 8). However, some of the differences between this study and Waring et al. (1979) can be attributed to differences in stand structure, climate and soil hydraulic properties between Brasschaat and the Scottish forest. For example, although basal area was roughly similar for the two study sites, the Scottish pine stand was younger (42 years old) and had a higher LAI. Also solar radiation during their study period is not known. Twenty years of water balance data from a younger (37 years old) Scots pine stand of similar basal area, higher LAI, but slightly lower radiation in central Germany had results similar to those reported here (Jaeger and Kessler, 1997). From their monthly averages, a mean daily ET of almost 1 mm day^{-1} was calculated in January to a little over 3 mm day^{-1} in July. These estimates were similar in magnitude to simulations from SECRETS (Fig. 8).

4.3. WAVE versus SECRETS

Evapotranspiration estimates from WAVE were often, but not always, higher than those simulated by SECRETS (especially during high water flux periods) and certainly those estimated from the eddy covariance approach (Figs. 8 and 9). A possible explanation why the WAVE estimates were generally higher is the fact that the depth of the clay substrate at the calibration point was rather shallow (125 cm). This likely created locally a more favourable soil moisture profile for root water uptake. Previous research on the diurnal courses of transpiration measured by sap flow (Meiresonne et al., 1999) has indicated that the amount and timing of rainfall affect WAVE estimates of transpiration. WAVE often estimated zero transpiration when rainfall was more than 1 mm d^{-1} and fell during a non-transpiring period (evening, night, early morning). The same phenomenon occurred when rainfall occurred during the day, but in a shorter period, so that the radiation sum was not affected. Meiresonne et al. (1999) also observed that simulations for rainy days were not as affected when the rainfall originated from a brief shower or when the rainfall persisted during the major part of the day.

Because the WAVE model uses daily values, it could not reproduce such events.

For days with any measurable rainfall, SECRETS always estimates canopy interception (or evaporation) by foliage and stems/branches (data not shown). And, some interception or evaporation from the soil surface litter often occurs (depending on whether rainfall exceeds interception and the potential evapotranspiration). Evaporation from the bare soil or transpiration may, or may not, occur during days with rain, depending on photosynthesis for the day (and thus canopy conductance), and long-wave radiation reaching the soil surface. Radiation at the soil surface depends on LAI, solar angle and, of course, incident radiation above the canopy. In SECRETS, at low to moderate ET, the water flux attributed to canopy interception (or evaporation) was proportionally higher than the other fluxes, while at higher ET, transpiration and, to a lesser extent, soil evaporation contributed proportionally more to ET (data not shown). Thus, the convergence between SECRETS and WAVE for days with rainfall to days without rain can be, at least partially, attributed to the closer correspondence between the two models for transpiration when transpiration is the dominant water flux from the forest. It is not known to what extent soil evaporation may have contributed to these results.

4.4. Eddy covariance versus the models WAVE and SECRETS

The curvilinear relationship in evapotranspiration as observed between the model SECRETS (ET_S) and the eddy covariance measurements (ET_{EC}) for days without rain (Fig. 9) was not entirely unexpected. Results from a joint modelling effort showed, in general, similar trends (P.G. Jarvis, personal communication). At low soil water content the low estimate of ET by SECRETS can be attributed to the low soil evaporation. Higher estimates of ET at low fluxes for both models, when compared to the eddy covariance fluxes, can be explained by 'selective' underestimation of the flux during calm periods (Goulden et al., 1996). When compared to the eddy data for SECRETS, reduced ET at higher fluxes is attributed to

decreased transpiration and canopy interception/ evaporation as ET increased. A reduction in transpiration as ET increased may be a biological feed-forward response to increasing water loss. However interception/evaporation from the canopy is strictly due to the physical structure of the canopy (LAI and light transmission) in relation to incident radiation. When soil water content is sufficient ($> 10\%$) estimates of evapotranspiration by WAVE (ET_W) are not reduced, as the soil driven transpiration (T_W) is not affected.

5. Conclusions

The four approaches used in this study to estimate the water fluxes contributing to evapotranspiration from a Scots pine forest differ in their process formulation and/or measurement scale in their flux estimates. Yet, the convergence between measured and modelled fluxes was interesting and often close, depending on the time resolution of the flux comparison made. Namely, the two simulation models had similar seasonal trends in transpiration; they had similar annual estimates of transpiration and soil evaporation. Evaporation in SECRETS generated more zero values, in drought events. Daily estimates of transpiration from SECRETS were well correlated with the sap flow estimates, but further fine-tuning and calibration of this model could be made. Estimates of transpiration from WAVE showed more over- and under estimations, as this model was more sensitive to rain events. The eddy covariance flux measurements (for days without precipitation) yielded lower evapotranspiration (ET) values then both models. The WAVE model simulated highest ET during summer, with peaks of nearly 5 mm d^{-1}, while SECRETS estimated higher ET during other times of the year.

Each of the four approaches has their own specific benefits and shortcomings for the assessment of water fluxes of a stand. The WAVE model needs easy to generate weather data and the knowledge of the soil properties as input. On the other hand, the modelling output is only a point simulation. The model SECRETS also relies on weather data, however canopy measurements are also required. The sap flow method offers a direct

measurement of the transpiration, but the up-scaling process can cause bias and error. The eddy covariance measurement is also a direct measurement of evapotranspiration fluxes, but it requires a tower infrastructure and it introduces uncertainty about the measured surface.

Appendix A. Description of the process model SECRETS (Sampson and Ceulemans 1999; Sampson et al. 2001)

(1) *Transpiration*

Transpiration in SECRETS (T_S) is determined by incident radiation (using Penman–Monteith) and leaf stomatal conductance to water vapor (g_s) (empirically estimated from photosynthesis). There are a series of equations used in the Penman–Monteith approach to calculate T_S. Net radiation (K_n; MJ m^{-2} day^{-1}) incident to the canopy surface is calculated from daily incident shortwave radiation. The equation to estimate K_n is:

$$K_n = (1 - a)K_s - K_{in} \tag{A1}$$

where: K_s is the daily value of total short-wave radiation (MJ m^{-2} day^{-1}), K_{in} the net long-wave radiation (MJ m^{-2} day^{-1}) and a is the albedo (proportional).

The model calculates K_{in} from average hourly temperature, estimated from minimum and maximum daily ambient air temperature (Sampson et al. 2001) and emissivity, as:

$$K_{in} = (0.1 + 0.9\, K_s/K_O)(\epsilon_a - \epsilon_v)\sigma(\text{temp} + 273)^4 \tag{A2}$$

where: ϵ_a is the emissivity of atmosphere, ϵ_v the emissivity of vegetation, σ the Stefan Boltzmann constant, temp is the average hourly temperature (°C) and K_O is the total (long-wave + short-wave) incoming radiation (MJ m^{-2} day^{-1}).

The apparent emissivity of atmosphere (ϵ_a) is calculated from hourly temperature as:

$$\epsilon_a = 1 - 0.261 \exp(-7.77 \times 10^{-4}\,\text{temp}^2) \tag{A3}$$

The heat transfer equations used in the Penman–Monteith approach depend, in part, on canopy conductance to estimate the imposed rate of transpiration. Canopy conductance is derived from g_s and LAI. We use the Ball and Berry approach (Ball et al., 1987) as adapted by Leuning (1995) to estimate g_s from hourly photosynthesis. Specifically, g_s (mol m^{-2} s^{-1}) is estimated as:

$$g_s = \delta_0 + B_1 \times A_n/((CO_{2c} - \Gamma) \times (1 + D/D_O)) \tag{A4}$$

where: δ_0 is the minimum cuticular conductance (mol m^{-2} s^{-1}), B_1 the empirical coefficient (μmol^{-1} m^2 s), A_n the net photosynthesis (μmol CO_2 m^{-2} s^{-1}), Γ is the CO_2 compensation point (Pa), D the vapour pressure deficit (Pa), D_O the saturation pressure (Pa), CO_{2c} is the CO_2 concentration in the canopy air (μmol mol^{-1}).

Details on the photosynthesis module may be found in de Pury and Farquhar (1997). The vapour pressure deficit is calculated hourly from temperature and relative humidity. Canopy conductance (G_C, mol m^{-2} ground s^{-1}), then, is integrated over the canopy as:

$$G_C = \int g_s\, dL \tag{A5}$$

where L is LAI (m^2 m^{-2}; projected area basis). LAI is a daily input into the model and was determined for this site using the LI-COR LAI-2000 Plant Canopy Analyzer adjusted to account for the self-shading of foliage elements within

shoots (shoot silhouette area < actual needle area of the shoot) (Stenberg 1996).

The instantaneous rate of canopy transpiration ($T_S(t)$; mm h^{-1}) depends on the equilibrium rate of transpiration, the imposed rate of transpiration, and the extent to that transpiration is determined by incident radiation versus canopy conductance (Jarvis 1985). The equilibrium rate of transpiration (T_{Seq}; mm h^{-1}) is calculated as:

$$T_{Seq} = sK_n/((s + \gamma)\lambda) \qquad (A6)$$

where: s is the slope of saturation vapour-pressure/temperature curve, γ the psychrometric coefficient (Pa °C^{-1}), λ is the latent heat of vaporization of water (J g^{-1}).

The imposed rate of transpiration (T_{Simp}; mm h^{-1}), then, is calculated as:

$$T_{Simp} = \rho C_p G_C \Delta e/(\lambda \gamma) \qquad (A7)$$

where: ρ is the partial pressure of dry air (kPa), C_p the specific heat capacity of air at constant pressure

(J g^{-1} °C^{-1}), Δe is the saturation vapour deficit of air (kPa).

The coupling coefficient (Ω) describes the extent to which $T_S(t)$ depends on K_n versus G_C and is estimated as:

$$\Omega = (s + \gamma)/s + \gamma + \gamma(G_b/G_C) \qquad (A8)$$

where G_b is canopy boundary layer conductance (mol m^{-2} s^{-1}) (see Table A1).

We calculate the instantaneous rate (mm h^{-1}) of canopy transpiration ($T_S(t)$) as:

$$T_S(t) = T_{Seq}\Omega + T_{Simp}(1 - \Omega) \qquad (A9)$$

Finally, daily transpiration (mm day^{-1}) is calculated as:

$$T_S = f_E \int T_S(t)\, dt \qquad (A10)$$

where f_E is the reduction of transpiration when canopy is partially wet.

(2) *Canopy (and tree bole) interception*

Canopy interception in SECRETS is determined

Table A1
Parameter list for soil water balance in SECRETS version 4.0

Parameter	Symbol	Units	Value	Reference
Canopy aerodynamic conductance	G_b	mol m^{-2} s^{-1}	6.027	Adapted from McMurtrie and Landsberg (1992)
Soil aerodynamic conductance	G_S	mol m^{-2} s^{-1}	0.5	Monteith (1973)
Soil diffusive conductance[a]	G_d	mol m^{-2} s^{-1}	0.4	Monteith (1973)
Albedo	a	Proportional	0.1	Default
Emissivity of vegetation	ϵ_v		0.95	Monteith and Unsworth (1990)
Minimum cuticular conductance	δ_0	mol m^{-2} s^{-1}	0.02	Medlyn and Jarvis (1999)
Stefan Boltzmann constant	σ	10–8 W m^{-2} K^{-4}	5.67	Monteith and Unsworth (1990)
CO$_2$ compensation point	Γ	Pa	3.69	de Pury and Farquhar (1997)
Slope coefficient for stomatal conductance	$B1$	μmol^{-1} m^2 s	4.8	Medlyn and Jarvis (1999)
Surface litter evaporation coeff.	α	mm	0.05	Adapted from Swank et al. (1972)
Profile sand content–top profile (0.2 m)	N.A.	%	78	Meiresonne and Overloop (1999)
Profile sand content–total profile (1.3 m)	N.A	%	83.9	Meiresonne and Overloop (1999)
Profile clay content–top profile (0.2 m)	N.A.	%	10	Meiresonne and Overloop (1999)
Profile clay content–total profile (1.3 m)	N.A.	%	6.7	Meiresonne and Overloop (1999)
Total profile depth	N.A.	m	1.3	Meiresonne and Overloop (1999)
Depth first layer	N.A.	m	0.2	Meiresonne and Overloop (1999)
LAI evaporation coefficient	EVAP$_L$	mm m^2 m^{-2}	0.5	Swank et al. (1972)
Stem flow coefficient	B	m^{-1}	0.1835	Loustau et al. (1992a)
Specific leaf area	psla	cm^2 g^{-1}	38.6	Smolander and Stenberg (1996)

Parameter estimates listed here include those used in the Penman–Monteith equations provided in the appendix text above as well as those pertaining to the stand soil characteristics. Parameters not listed here but found in the appendix text above were either estimated by the model during simulations or were constants.

[a] Assumed proportional to soil water content of the top soil layer.

by LAI, average tree diameter at breast height (dbh; m) and incident radiation. For days with precipitation events, the interception of precipitation by foliage is calculated as the minimum estimate between that derived empirically, and that estimated from Penman–Monteith.

The empirical estimate, from LAI, is:

$$E_{i,S} = (L \times EVAP_L) \qquad (A11)$$

where $EVAP_L$ is the species evaporation coefficient (mm m^2 m^{-2}).

As mentioned, the model also uses an empirical estimate of the amount of precipitation intercepted by individual tree boles. This equation was adapted from Loustau et al. (1992a) and is defined as:

$$Stem\ Flow = Precip \times B \times dbh \qquad (A12)$$

where Precip is the precipitation (mm day^{-1}), B the empirical coefficient (m^{-1}), dbh is the average tree diameter at breast height (m).

The total amount of daily precipitation (for precipitation events) intercepted is the summation of that intercepted by foliage and stems.

(3) *Evaporation*

Evaporation of precipitation from the surface litter (mm day^{-1}) is derived in a similar fashion as that from the wet foliated canopy. Namely, it is defined as the minimum between that estimated empirically, as determined by the mass of surface litter, and that estimated from the Penman–Monteith equations.

The empirical estimate is:

$$E_{l,S} = (LIT_{surf} \times psla)/10 \times \alpha \qquad (A13)$$

where LIT_{surf} is the surface litter (kg m^{-2}), psla the projected specific leaf area (cm^2 g^{-1}), α is a constant (mm).

Evaporation of water from the soil profile depends on the Penman–Monteith equations described above with obvious changes in the input parameters. Namely, dependencies of Ω use soil aerodynamic conductance (G_S) and soil diffusive conductance (G_d) instead of the comparable canopy parameters. In a similar fashion, the imposed rate of evaporation also depends on G_d. Parameters and parameter estimates used in the equations discussed above may be found in Table A1.

References

Aubinet, M., Grelle, A., Ibrom, A., Rannik, Ü., Moncrieff, J., Foken, T., Kowalski, A.S., Martin, P.H., Berbigier, P., Bernhofer, Ch., Clement, R., Elbers, J., Granier, A., Grünwald, T., Morgenstern, K., Pilegaard, K., Rebmann, C., Snijders, W., Valentini, R., Vesala, T., 2000. Estimates of the annual net carbon and water exchange of forests: the EUROFLUX methodology. Advances in Ecological Research 30, 113–173.

Baldocchi, D.D., Vogel, C.A., 1996. Energy and CO2 flux densities above and below a temperate broad-leaved forest and a boreal pine forest. Tree Physiology 16, 5–16.

Baldocchi, D.D., Valentini, R., Running, S., Oechel, W., Dahlman, R., 1996. Strategies for measuring and modelling carbon dioxide and water vapour fluxes over terrestrial ecosystems. Global Change Biology 3, 159–168.

Ball, J.T., Woodrow, I.E., Berry, J.A., 1987. A model predicting stomatal conductance and its contribution to the control of photosynthesis under different environmental conditions, In: Biggins, J., (Ed.), Progress in Photosynthesis Research, vol. IV. Martinus Nijhoff, Dordrecht, The Netherlands, pp. 221–224.

Berbigier, P., Bonnefond, J.M., Loustau, D., Ferreira, M.I., David, J.S., Pereira, J.S., 1996. Transpiration of a 64-year-old maritime pine stand in Portugal. 2. Evapotranspiration and canopy stomatal conductance measured by an eddy covariance technique. Oecologia 107, 43–52.

Berninger, F., 1997. Effects of drought and phenology on GPP in *Pinus sylvestris*. A simulation study along a geographical gradient. Functional Ecology 11, 33–42.

Calder, I.R., 1977. A model of transpiration and interception loss from a spruce forest in Plynlimon, central Wales. Journal of Hydrology 33, 247–265.

Calder, I.R., 1986. A stochastic model of rainfall interception. Journal of Hydrology 124, 119–130.

Cermák, J., 1989. Solar equivalent leaf area: an efficient biometrical parameter of individual leaves, trees and stands. Tree Physiology 5, 269–289.

Cermák, J., Kucera, J., 1987. , Transpiration of fully grown trees and stands of spruce (*Picea abies* (L.) Karst.) estimated by the tree-trunk heat balance method,In: Swanson, R.H., Bernier, P.Y., Woodward, P.D. (Eds.), Proceedings of Forest Hydrology and Watershed Measurements, Vancouver, Canada, IAHS-AISH Publ. no. 167, Wallingford, UK, pp. 311–317.

Cermák, J., Kucera, J., 1990. Scaling up transpiration data between trees, stands and watersheds. Silva Carelica 15, 101–120.

Cermák, J., Michalek, J., 1991. Selection of sample trees in forest stands using the quantils of total. Lesnictvi/Forestry 37, 49–60.

Cermák, J., Nadezhdina, N., 1998. Sapwood as the scaling parameter-defining according to xylem water content or radial pattern of sap flow? Annals of Forest Sciences 55, 509–521.

Cermák, J., Riguzzi, F., Ceulemans, R., 1998. Scaling up from the individual tree to the stand level in Scots pine. I. Needle distribution, overall crown and root geometry. Annals of Forest Science 55, 63–88.

Cermák, J., Kucera, J., Prax, A., Tatarinov, F., Nadezhdin, V., 2001. Long-term course of transpiration in a floodplain forest in

southern Moravia associated with changes of underground water table. Ekologia 20, 92–115.

Ceulemans, R., Kowalski, A.S., Berbigier, P., Dolman, H., Elbers, J., Grelle, A., Janssens, I.A., Lindroth, A., Moors, E., Rannik, U., Vesala, T., 2002. carbon and water fluxes of pine (*Pinus*) forests: their balances, ecological and ecophysiological Determinants, In: Valentini, R., (Ed.), Ecological Studies: Fluxes of Carbon, Water and Energy of European Forests, Springer, Berlin, in press.

Chiesi, M., Maselli, F., Bindi, M., Fibbi, L., Bonora, L., Raschi, A., Cermák, J., Nadezhdina, N., 2002. Calibration and application of forest-BCG in a Mediterraen area by the use of conventional and remote sensing data. Ecological Modelling 154, 251–262.

Cienciala, E., Kucera, J., Lindroth, A., Cermák, J., Grelle, A., Halldin, S., 1997. Canopy transpiration from a boreal forest in Sweden during a dry year. Agricultural and Forest Meteorology 86, 157–167.

Dekker, S.C., Bouten, W., Verstraten, J.M., 2000. Modelling forest transpiration from different perspectives. Hydrological Processes 14, 251–260.

Galmarini, S., Thunis, P., 1999. On the validity of Reynolds assumptions for running-mean filters in the absence of a spectral gap. Journal of the Atmospheric Sciences 56, 1785–1796.

Gardner, W., 1958. Some steady state solutions of the unsaturated moisture flow equation with application to evaporation from a water table. Soil Science 85, 228–232.

Gash, J.H.C., 1979. An analytical model of rainfall interception by forests. Quarterly Journal of the Royal Meteorological Society 105, 43–55.

Gellens-Meulenberghs, F., Gellens, D., 1992. L'évapotranspiration potentielle en Belgique: variabilité spatiale et temporelle. Institut Royal Météorologique de Belgique, Publications, Série A 130.

Gond, V., de Pury, D.G.G., Veroustraete, F., Ceulemans, R., 1999. Seasonal variation in leaf area index, leaf chlorophyll, and water content; scaling-up to estimate fAPAR and carbon balance in a multilayer, multispecies temperate forest. Tree Physiology 19, 673–679.

Goulden, M.L., Munger, J.W., Fan, S.-M., Daube, B.C., Wofsy, S.C., 1996. Measurements of carbon sequestration by long-term eddy covariance: methods and a critical evaluation of accuracy. Global Change Biology 2, 169–182.

Granier, A., Biron, P., Lemoine, D., 2000. Water balance, transpiration and canopy conductance in two beech stands. Agricultural and Forest Meteorology 100, 291–308.

Hatton, T.J., Moore, S.J., Reece, P.H., 1995. Estimating stand transpiration in *Eucalyptus populnea* woodland with the heat pulse method: measurement errors and sampling strategies. Tree Physiology 4, 219–227.

Hubrechts, L., Van de Moortel, R., Feyen, J., 1997. Berekening van de bodemwaterbalans onder bos voor de proefvlakken van het Bosbodemmeetnet Vlaanderen (periode: 1990–1995), Internal publication nr.47, Institute for Land and Water Management, Catholic University of Leuven, p. 122, in Dutch.

Irvine, J., Perks, M.P., Magnani, F., Grace, J., 1998. The response of *Pinus sylvestris* to drought: stomatal control of transpiration and hydraulic conductance. Tree Physiology 18, 393–402.

Item, H., 1978. A model for the water regime of coniferous forest and grassland. Journal of Hydrology 37, 323–332.

Jaeger, L., Kessler, A., 1997. Twenty years of heat and water balance climatology at the Hartheim pine forest, Germany. Agricultural and Forest Meteorology 84, 25–36.

Janssens, I.A., Sampson, D.A., Cermák, J., Meiresonne, L., Riguzzi, F., Overloop, S., Ceulemans, R., 1999. Above-and below-ground phytomass and carbon storage in a Belgian Scots pine stand. Annals of Forest Science 56, 81–90.

Jarvis, P., 1985. Transpiration and assimilation of tree and agricultural crops: the OMEGA Factor, In: Cannell, M.G.R., Jackson, J.E. (Eds.), Trees as Crop Plants, Institute of Terrestrial Ecology, Edinburgh, p. 460.

Jarvis, P.G., 1995. Scaling processes and problems. Plant Cell and Environment 18, 1079–1089.

Jimenez, M.S., Cermák, J., Kucera, J., Morales, D., 1996. Laurel forests in Tenerife, Canary Islands: the annual course of sap flow in *Laurus* trees and stand. Journal of Hydrology 183, 305–319.

Kostner, B., Granier, A., Cermák, J., 1998. Sap flow measurements in forest stands-methods and uncertainties. Annales des Sciences Forestières 55, 13–27.

Kowalski, A.S., Overloop, S., Ceulemans, R., 1999. Eddy fluxes above a Belgian, Campine forest and relationships with predicting variables, In: Ceulemans, R.J.M., Veroustraete, F., Gond, V., Van Rensbergen, J.B.H.F. (Eds.), Forest Ecosystem Modelling, Upscaling and Remote Sensing, SPB Academic Publishing, The Hague, The Netherlands, pp. 3–18.

Leuning, R., 1995. A critical appraisal of a combined stomatal-photosynthesis model for C_3 plants. Plant Cell and Environment 18, 339–355.

Leyton, L., Reynolds, E.R.C., Thompson, F.B., 1967. Rainfall interception in forest and moorland, In: Sopper, W.E., Lull, H.W. (Eds.), International Symposium on Forest Hydrology, Pergamon Press, Oxford, UK, pp. 163–178.

Loustau, D., Berbigier, P., Granier, A., El Hadj Moussa, F., 1992a. Interception loss, throughfall and stemflow in a maritime pine stand. I. Variability of throughfall and stemflow beneath the pine canopy. Journal of Hydrology 138, 449–467.

Loustau, D., Berbigier, P., Granier, A., 1992b. Interception loss, throughfall and stemflow in a maritime pine stand. II. An application of Gash's analytical model of interception. Journal of Hydrology 138, 469–485.

Loustau, D., Berbigier, P., Roumagnac, P., Arruda-Pacheco, C., David, J.S., Ferreira, M.I., Pereira, J.S., Tavares, R., 1996. Transpiration of a 64-year-old maritime pine stand in Portugal. 1. Seasonal course of water flux through maritime pine. Oecologia 107, 33–42.

Lundblad, M., Lagergren, F., Lindroth, A., 2001. Evaluation of heat balance and heat dissipation methods for sapflow measurements in pine and spruce. Annals of Forest Science 58, 625–638.

Martin, T.A., Brown, K.J., Kucera, J., Meinzer, F.C., Sprugel, D.G., Hinckley, T.M., 2001. Control of transpiration in a 220-year-old *Abies amabilis* forest. Forest Ecology and Management 152, 211–224.

McMillen, R.T., 1988. An eddy correlation technique with extended applicability to non-simple terrain. Boundary-Layer Meteorology 43, 231–245.

McMurtrie, R.E., Landsberg, J.J., 1992. Using a simulation model to evaluate the effects of water and nutrients on the growth and carbon partitioning of *Pinus radiata*. Forest Ecology and Management 52, 243–260.

McNaughton, K.G., Jarvis, P.G., 1983. Predicting the effects of vegetation changes on transpiration and evaporation, In: Kozlowski, T.T., (Ed.), Water Deficits and Plant Growth, vol. VII. Academic Press, New York, pp. 1–47.

Medlyn, B.E., Jarvis, P.G., 1999. Design and use of a database of model parameters from elevated CO_2 experiments. Ecological Modelling 124, 69–83.

Meiresonne, L., Nadezhdina, N., Cermak, J., Van Slycken, J., Ceulemans, R., 1999. Measured sap flow and simulated transpiration from a poplar stand in Flanders (Belgium). Agricultural and Forest Meteorology 96, 165–179.

Meiresonne, L., Overloop, S., 1999. Transpiratiebegroting van een Grove dennenbestand: een eerste modelmatige benadering, Communications of The Institute for Forestry and Game Management no.1999/1, pp. 103–119.

Milne, R., Deans, J.D., Ford, E.D., Jarvis, P.G., Leverenz, J., Whitehead, D., 1985. A comparison of two methods of estimating transpiration rates from a Sitka spruce plantation. Boundary-Layer Meteorology 32, 155–175.

Moncrieff, J.B., Massheder, J.M., De Bruin, H., Elbers, J., Friborg, T., Heusinkveld, B., Kabat, P., Scott, S., Soegaard, H., Verhoef, A., 1997. A system to measure surface fluxes of momentum, sensible heat, water vapour and carbon dioxide. Journal of Hydrology 188–189, 589–611.

Monteith, J.L., 1965. Evaporation and the environment, The State and Movement of Water in Living Organisms. XIX Symposium Society for Experimental Biology, Swansea, pp. 205–234.

Monteith, J.L., 1973. Principles of Environmental Physics, Edward Arnold, London, UK, p. 241.

Monteith, J.L., Unsworth, M., 1990. Principles of Environmental Physics, second ed., Edward Arnold, London, UK, p. 291.

Nadezhdina, N., Cermák, J., Nadezhdin, V., 1998. Heat field deformation method for sap flow measurements. Proceedings Fourth International Workshop on Measuring Sap Flow in Intact Plants. Zidlochovice, Czech Republic, October 3–5, 1998. IUFRO Publications. Publishing house of Mendel University of Brno, pp. 72–92.

Nadezhdina, N., 1999. Sap flow index as an indicator of plant water status. Tree Physiology 19, 885–891.

Nadezhdina, N., Cermák, J., 1999. The technique and instrumentation for estimation the sap flow rate in plants. Patent No.286438, A 01G 7/00 (PV-1587-98; US Patent and Trademark Rec. No. 69055, 1997), Vestnik 19/1999, p. 47.

Nadezhdina, N., Cermák, J., Tributsch, H., 2000. Heat field around the linear heater used for sap flow measurement by the HFD-method as observed by the infra-red camera, In: Raschi, A., (Ed.), Fifth International Workshop on Measuring Sap Flow in Intact Plants, Firenze, Italy, p. 10.

Nadezhdina, N., Nadezhdin, V., 2001. Variation of sap flow and conducting pathways in tree stems as detected by radial pattern sensors, In: Vesala, T., (Ed.), Water Transport in woody plants and linkages to plant structure and productivity. Workshop in

Hytiala Forest Station, Finland (Magnus Ehrnrooth Foundation), p. 16.

Nadezhdina, N., Cermák, J., Morales, D., Jimenez, M.S., Raschi, A., Ferreira, I., Michaelsen, J., 2001. Variations in conducting patterns of trees growing in three mediterraen countries and relations to crown development, In: Radoglou, K., (Ed.), International Conference on Forest Research: A Challenge for an Integrated European Approach, Thesalonniki, Greece, vol. 2., pp. 507–512.

Nadezhdina, N., Cermák, J., Ceulemans, R., 2002. Radial pattern of sap flow in woody stems related to positioning of sensors and scaling errors in dominant and understorey species. Tree Physiology 22, 907–918.

Overloop, S., Meiresonne, L., 1999. Basiskarakteristieken van het proefvlak Brasschaat, domeinbos de Inslag, Communications of The Institute for Forestry and Game Management no. 1999/1, pp. 11–21, in Dutch.

de Pury, D.G.G., Ceulemans, R., 1997. Scaling-up carbon fluxes from leaves to stands in a patchy coniferous/deciduous forest, In: Mohren, G.M.J., Kramer, K., Sabate, S. (Eds.), Impacts of Global Change on Tree Physiology and Forest Ecosystems, Kluwer, The Netherlands, pp. 263–272.

de Pury, D.G.G., Farquhar, G.D., 1997. Simple scaling of photosynthesis from leaves to canopies without the errors of big-leaf models. Plant Cell and Environment 20, 537–557.

Raupach, M.R., Finnigan, J.J., 1988. Single-layer models of evaporation from plant canopies are incorrect, but useful, whereas multilayer models are correct but useless. Australian Journal of Plant Physiology 15, 705–716.

Richards, L.A., 1931. Capillary conduction of liquid through porous medium. Physics 1, 318–333.

Roskams, P., Sioen, G., Overloop, S., 1997. Meetnet voor de intensieve monitoring van het bosecosysteem in het Vlaamse Gewest-Resultaten 1991–1992, Flemish Community, Institute for Forestry and Game Management, Belgium, pp. 41–66, in Dutch.

Rutter, A.J., Keshaw, K.A., Robins, P.C., Morton, A.J., 1971. A predictive model of rainfall interception in forests. I. Derivation of the model from observations in a plantation of Corsican pine. Agricultural and Forest Meteorology 9, 367–384.

Rutter, A.J., Morton, A.J., Robins, P.C., 1975. A predictive model of rainfall interception by forests. II. Generalization of the model and comparison with observations in some coniferous and hardwood stands. Journal of Applied Ecology 12, 367–381.

Sampson, D.A., Ceulemans, R., 1999. SECRETS: Simulated carbon fluxes from a mixed coniferous/deciduous Belgian forest, Forest Ecosystem Modelling, In: Ceulemans, R.J.M., Veroustraete, F., Gond, V., Van Rensbergen, J.B.H.H. (Eds.), Upscaling and Remote Sensing, SPB Academic Publishing, The Hague, The Netherlands, pp. 95–108.

Sampson, D.A., Janssens, I.A., Ceulemans, R., 2001. Simulated soil CO_2 efflux and net ecosystem exchange in a 70-year-old Belgian Scots pine stand using the process model SECRETS. Annals of Forest Science 58, 31–44.

Saxton, K.E., Rawls, W.J., Romberger, J.S., Papendick, R.I., 1986. Estimating generalized soil-water characteristics from texture. Soil Science Society of America Journal 50, 1031–1036.

Smolander, H., Stenberg, P., 1996. Response of LAI-2000 estimates to changes in plant surface area index in a Scots pine stand. Tree Physiology 16, 345–349.

Stenberg, P., 1996. Correcting LAI-2000 estimates for the clumping of needles in shoots of conifers. Agricultural and Forest Meteorology 79, 1–8.

Stewart, J.B., 1984. Measurement and prediction of evaporation from forested and agricultural catchments. Agricultural Water Management 8, 1–28.

Stewart, J.B., 1988. Modelling surface conductance of pine forest. Agricultural and Forest Meteorology 43, 19–35.

Swank, W.T., Goebel, N.B., Helvey, J.D., 1972. Interception loss in loblolly pine stands of the South Carolina piedmont. Journal of Soil Water Conservation 27, 160–164.

Thornley, J.M., 1998. Grasslands Dynamics: an ecosystem simulation model, CAB International, Wallingford, UK, p. 241.

Valentini, R., Matteucci, G., Dolman, A.J., Schulze, E.D., Rebmann, C., Moors, E.J., Granier, A., Gross, P., Jensen, N.O., Pilegaard, K., Lindroth, A., Grelle, A., Bernhofer, C., Grünwald, T., Aubinet, M., Ceulemans, R., Kowalski, A.S., Vesala, T., Rannik, U., Berbigier, P., Loustau, D., Guömunndson, J., Thorgeirsson, H., Ibrom, A., Morgenstern, K., Clement, R., Moncrieff, J., Montagnani, L., Minerbi, S., Jarvis, P.G., 2000. Respiration as the main determinant of carbon balance in European forests. Nature 404, 861–865.

Vanclooster, M., Viaene, P., Diels, J., Christiaens, K., 1994. WAVE, a mathematical model for simulating water and agrochemicals in the soil and vadose environment. Reference and User's Manual, Institute for Land and Water Management, Catholic University of Leuven, pp. 144.

Van Den Berge, K., Maddelein, D., De Vos, B., Roskams, P., 1992. Analyse van de luchtverontreiniging en de gevolgen daarvan op het bosecosysteem, Report no. 19 of AMINAL, Ministry of the Flemish Community, p. 169, in Dutch.

van Genuchten, M.Th., 1980. A closed-form equation for predicting the hydraulic conductivity of soil. Soil Science Society of America Journal 44, 892–898.

Van Slycken, J., Van Ranst, E., De Coninck, F., 1997. In: Roskams, P., Sioen, G., Overloop, S. (Eds.), Profielbeschrijving en textuur. Meetnet voor de intensieve monitoring van het bosecosysteem in het Vlaamse Gewest-Resultaten 1991–1992, Flemish Community, Institute for Forestry and Game Management, Belgium, pp. 41–66, in Dutch.

Verstraeten, W.W., Minnaert, M., Meiresonne, L., Lemeur, R., De Vos, B., Van Slycken, J., Deckers, J., Muys, B., Feyen, J., 2001. Kwantitatieve analyse van de verdamping van bossen in vergelijking met weide en akkerland, VLINA-9906, p.225, in Dutch.

Vickers, D., Mahrt, L., 1997. Quality control and flux sampling problems for tower and aircraft data. Journal of Atmospheric and Oceanic Technology 14, 512–526.

Waring, R.H., Whitehead, D., Jarvis, P.G., 1979. The contribution of stored water to transpiration in Scots pine. Plant Cell and Environment 2, 309–317.

Wilson, K.B., Hanson, J.H., Mulholland, P.J., Baldocchi, D.D., Wullschleger, S.D., 2001. A comparison of methods for determining forest evapotranspiration and its components: sap-flow, soil water budget, eddy covariance and catchment water balance. Agricultural and Forest Meteorology 106, 153–168.